Magneto-optical properties of $Zn_{0.95}Mn_{0.05}Se/Zn_{0.76}Be_{0.08}Mg_{0.16}Se$ quantum wells and $Zn_{0.91}Mn_{0.09}Se/Zn_{0.972}Be_{0.028}Se$ spin superlattices

B. König, U. Zehnder, D. R. Yakovlev,* W. Ossau, T. Gerhard, M. Keim, A. Waag, and G. Landwehr
Physikalisches Institut der Universität Würzburg, Am Hubland, D-97074 Würzburg, Germany
(Received 22 February 1999)

We have performed magnetoluminescence and magnetoreflectance studies on novel semimagnetic semiconductor heterostructures based on (ZnMn)Se/(ZnBeMg)Se. The successful fabrication and various optical properties of that system are demonstrated by $Zn_{0.95}Mn_{0.05}Se/'' ''Zn_{0.76}Be_{0.08}Mg_{0.16}Se$ single quantum wells. The exciton spin splitting was used to determine the valence-band offset for (ZnMn)Se/(ZnBeMg)Se to 0.22 of the total band-gap discontinuity. Weakly confining multiple quantum wells made of $Zn_{0.91}Mn_{0.09}Se/Zn_{0.972}Be_{0.028}Se$ demonstrate a change of the band alignment from type I to type II for one of the exciton spin components in external magnetic fields which results in the formation of a spin superlattice. This spin superlattice formation manifests itself in an asymmetric Zeeman splitting of a spatially direct exciton caused by a spin-dependent change of the exciton binding energy. A pronounced broadening of the exciton in reflectance and photoluminescence excitation spectra was observed when scattering into the (ZnBe)Se barriers becomes possible. [S0163-1829(99)01028-0]

I. INTRODUCTION

In the past decade, II-VI semiconductors based on ZnSe have attracted great attention both for basic research and for its application as optoelectronic devices for the blue-green spectral range.[1] Diluted magnetic semiconductor (DMS) [e.g., (ZnMn)Se] are of special interest due to remarkable magnetic properties displayed by such a system. They stem from a strong $s,p-d$ exchange interaction between the electron and hole states and the localized states of Mn^{2+} $3d$ electrons and lead to peculiar optical properties such as giant Zeeman splittings of magnetoexcitons.[2] The use of DMS in nanostructures has brought a lot of new and interesting phenomena in the physics of low-dimensional systems. Thus confining potentials for carriers are tunable by external magnetic fields, which allows us to realize a transition from a type I to a type II band alignment and to form a spin superlattice. In addition, the magnetic polaron formation was shown to be drastically modified by the localization of carriers in quantum wells.[3,4]

The main problem of existing semimagnetic semiconductor heterostructures based on ZnSe such as (ZnMn)Se/ZnSe is to achieve strong carrier confinement while maintaining structural quality and a sufficient Mn content ($5-10\,\%$). For this system the bowing of the band gap for low Mn concentrations implies $Zn_{1-x}Mn_xSe$ to form the well for $x<0.05$ only with a total band-gap dicontinuity smaller than 150 meV.[5] At higher Mn fractions ($x>0.05$) $Zn_{1-x}Mn_xSe$ is the barrier material and a larger confinement can be attained on the expense of a reduced overlap of the carrier wave functions with the Mn system. Up to now, efforts to overcome this restriction succeeded only by involving a quaternary alloy like (ZnCdMn)Se as a quantum-well material,[6] which in turn leads to additional alloy broadening of the excitonic states.

The application of Be chalcogenides as new barrier materials for ZnSe has proven to be of great potential. Thus compounds, such as (ZnBeMg)Se, can be grown lattice matched on GaAs substrates with high Be concentrations with a band gap up to about 4 eV.[7] This is in contrast to previously used (ZnMg)Se, where strain limits the Mg content (and hence the band gap) to a few percent for the growth on GaAs substrates. Recently first laser emission of diode structures containing (ZnBeMg)Se barriers has been reported.[8] Concerning its favorable properties, (ZnBeMg)Se represents also an ideal barrier material for (ZnMn)Se wells that allows tuning of band offsets in a wide range.

The concept of a spin superlattice (SSL) was first proposed by von Ortenberg[9] as a system of alternating magnetic and nonmagnetic layers with vanishing valence- and conduction-band offset. With applied magnetic fields the large Zeeman splitting of band states in the magnetic layers leads to a spatial separation of carriers with different spin components. In the case of nonvanishing band offsets, which is most common in real systems, this spin-dependent carrier separation occurs for electrons and/or holes at finite magnetic fields when the Zeeman splitting exceeds the respective band offset. Consequently, the additional formation of spatially indirect excitons is expected in these layers. Until now, properties of SSLs have been investigated for various combinations of magnetic and nonmagnetic materials [e.g., (CdMg)Te/(CdMn)Te,[10] ZnSe/(ZnMn)Se,[11] ZnSe/(ZnFe)Se (Ref. 12)] and also for heterostructures consisting of two different DMSs such as (ZnFe)Se/(ZnMn)Se (Ref. 13) that distinguish in their individual magnetic properties.

In this paper we present results on successful fabrication and optical study of type I (ZnMn)Se/(ZnBeMg)Se single quantum wells (QWs) and (ZnMn)Se/(ZnBe)Se multiple quantum wells (MQWs) as a new representative for spin superlattices.

II. EXPERIMENTALS

The samples under investigation were grown by molecular-beam epitaxy (MBE) in a Riber system on (001)-

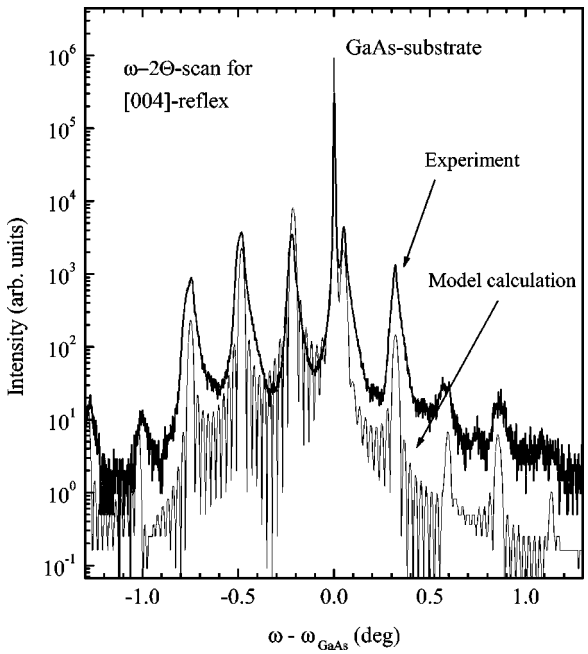

FIG. 1. X-ray-diffraction spectrum of a 100 Å/100 Å $Zn_{0.91}Mn_{0.09}Se/Zn_{0.972}Be_{0.028}Se$ superlattice (sample *B*) with the corresponding simulation.

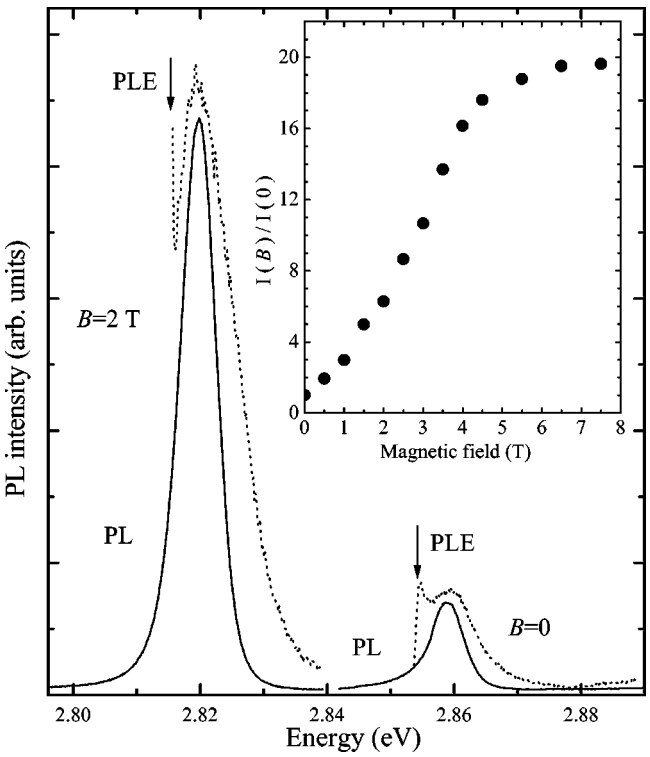

FIG. 2. PL (solid lines) and PLE spectra (dotted lines) of a 52-Å-thick $Zn_{0.95}Mn_{0.05}Se/''\,''Zn_{0.76}Be_{0.08}Mg_{0.16}Se$ QW (sample *A*) for $B=0$ and 2 T at a temperature of 1.7 K. Inset: Magnetic-field dependence of the integral PL intensity $I(B)$ normalized to the zero-field intensity $I(0)$ determined for excitation below the barrier energy in Faraday geometry.

oriented GaAs substrates. Prior to the growth of the layers, a 4-ML-thick BeTe buffer was deposited in order to improve the surface quality. Sample *A* contains two $Zn_{0.95}Mn_{0.05}Se$ QWs of thickness $L_z=52$ Å and 15 Å embedded in 1000-Å-thick barriers made of $Zn_{0.76}Be_{0.08}Mg_{0.16}Se$. The inner barrier which separates the quantum wells is 250 Å thick. Our multiple quantum well (sample *B*) consists of 20 periods of alternating 100-Å-thick layers of $Zn_{0.91}Mn_{0.09}Se$ and $Zn_{0.972}Be_{0.028}Se$.

Composition and structural quality of the samples were examined by x-ray diffraction. As an example, we demonstrate in Fig. 1 the rocking curve ($\omega-2\Theta$ scan) of sample *B* revealing a feature of the GaAs substrate and equidistant satellite peaks of the (ZnBe)Se/(ZnMn)Se SL. The increased broadening of the satellite peaks with higher order reflects a small drift either in compositon or layer thicknesses. A dynamical theory of diffraction[14] has been used to simulate the spectrum (thin curve in Fig. 1) and to determine the sample parameters as given above within an error of about 10%.

Optical spectra were taken at different sample temperatures ranging from 1.7 K (pumped liquid helium) up to 34 K. Magnetic fields up to 7.5 T, generated by a superconducting split-coil solenoid, were applied parallel to the growth axis (Faraday geometry). An Ar-ion laser served as the excitation source for photoluminescence (PL) or as a pump source for a tunable dye laser (Stilben 3) used in PL excitation (PLE) experiments. For reflectance measurements a halogen lamp was applied. The circular polarized signal was analyzed by a 1-m monochromator and detected with a charged-coupled-device (CCD) or a cooled photomultiplier tube followed by a photon-counting system.

III. RESULTS AND DICUSSION

A. Single-quantum-well structure

For the 52-Å-thick QW of sample *A*, the PL and PLE spectra taken under excitation below the energy of the barrier band gap are shown in Fig. 2 for zero magnetic field and 2 T. The heavy-hole exciton (X_{hh}) with an energy of 2.86 eV at $B=0$ gives the strongest signals in both spectra. No significant Stokes shift between PL and PLE has been observed, which gives evidence of a suppressed spectral diffusion in this structure and absence of the magnetic polaron formation. Apart from a giant splitting of about 50 meV at 7.5 T for each Zeeman branch, the spectra keep qualitatively unchanged in external magnetic fields. Nevertheless, even at $B>2$ T for which the luminescence is up to 90% σ^+-polarized, the PL intensity continues to increase strongly with the magnetic field. The overall increase of the integral intensity of the QW luminescence is about a factor of 20 (see the inset of Fig. 2). The laser energy used here was kept below the absorption edge of the barriers and of the 15-Å-thick QW to ensure a constant excitation power impinging on the considered layer. Only two mechanisms are conceivable for the intensity increase as the problem of carrier collection from the barrier into the QW is excluded by direct excitation of the QW. These are the suppression of the internal Mn^{2+} transition and the suppression of nonradiative recombination. For the investigated structure, the integral intensity of the internal Mn^{2+} transition is very weak at $B=0$ (15% of the integral QW luminescence) and reveals no measureable magnetic-field dependence. Thus the suppression of the exchange Auger process[15] (the channel for exciting Mn^{2+} ions) in magnetic fields can be neglected here. Consequently, we believe that a strong suppression of nonradiative recombination channels located in the magnetic

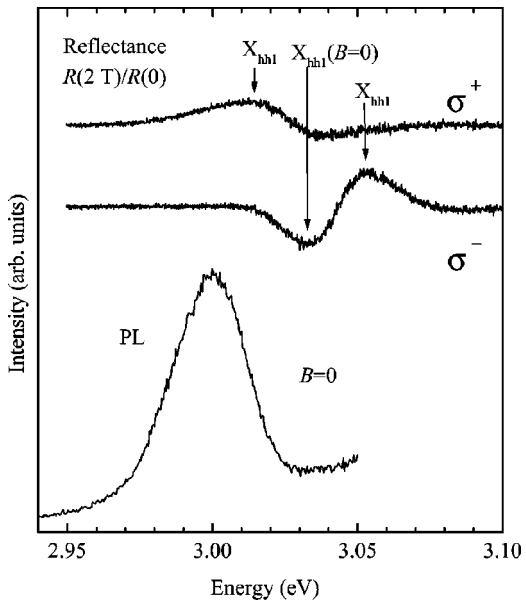

FIG. 3. Reflectance spectra $R(2\,\mathrm{T})/R(0)$ and zero-field PL spectrum (excited with a laser energy of 4.1 eV) of a 15-Å-thick $Zn_{0.95}Mn_{0.05}Se/Zn_{0.76}Be_{0.08}Mg_{0.16}Se$ QW (sample A) for $T=1.7$ K.

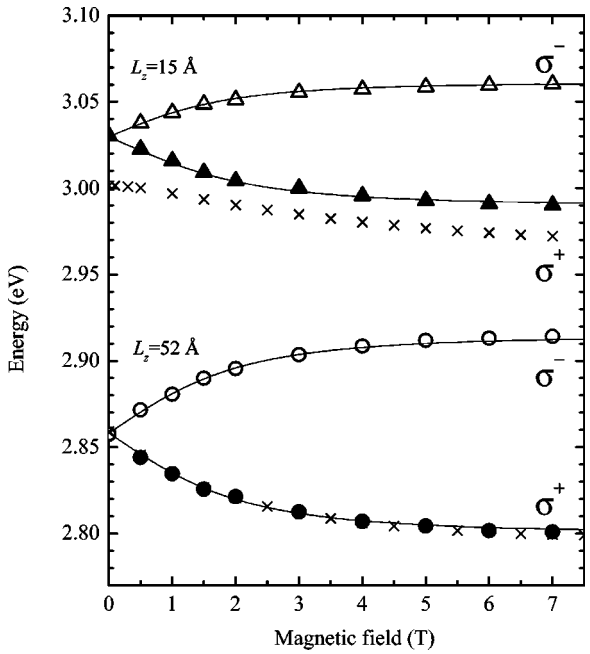

FIG. 4. Experimental heavy-hole exciton energies (X_{hh} line) with different spin components for two $Zn_{0.95}Mn_{0.05}Se/Zn_{0.76}Be_{0.08}Mg_{0.16}Se$ QW's vs magnetic-field strength taken from PL ($\times$), PLE ($\bigcirc$), and reflectance ($\triangle$) for σ^+ and σ^- polarization (closed and open symbols) at $T=1.7$ K. Solid lines represent model calculations of exciton energies.

layer is responsible for the drastic increase of the luminescence intensity. The special choice of excitation energy which has been necessary for a quantitative statement and the sample characteristic were found to be not crucial as a strong gain in PL intensity with magnetic field has also been observed under the condition of excitation above the barrier for both QWs of sample A and for the MQW (sample B). The barrier luminescence (only detected for sample A) undergoes no changes in magnetic fields, which implies a constant collection of carriers into the QWs. Moreover, the intensity increase is maintained for the magnetic field oriented parallel to the layers (Voigt geometry), which prevents a loss of carriers to surface states (with successive nonradiative recombination) to a high degree. It is left to understand the underlying process that suppresses nonradiative channels in (ZnMn)Se QW layers and reveals such a strong magnetic-field dependence.

The PL spectrum of the 15-Å-thick QW (Fig. 3) is rather broad due to a stronger influence of well-width fluctuations leading to a full width at half maximum (FWHM) of 33 meV, which is larger by 25 meV than for the wide QW. The luminescence has been excited with a laser energy of 4.1 eV, i.e., above the barrier absorption edge. Magnetic-field dependence of the free X_{hh} exciton was measured by reflectance R since the spectral range around 3.2 eV is not available for our dye laser. As a result of broadening, the exciton resonance does not appear as a pronounced feature in linear reflectivity spectra. Therefore, we have analyzed the ratio $R(B)/R(B=0)$ that indicates magnetic-field-induced modifications of the reflectance with respect to the zero-field signal by $R(B)/R(B=0)\neq 1$. The procedure is demonstrated in Fig. 3 for $B=2$ T, which yields resonances of the X_{hh} exciton as marked by arrows.

Experimental energies taken from PL (crosses), PLE (circles), and reflectance (triangles) spectra detected in σ^+ and σ^- polarization are plotted in Fig. 4 for both QWs of sample A. The maximum Zeeman splitting for the $L_z=15$ Å QW is about 25 meV smaller than for the broad QW with $L_z=52$ Å, which results from a larger penetration of the excitons wave function into the nonmagnetic barriers for the narrow QW.

By fitting theoretical exciton energies to our experimental ones simultaneously for both QWs, we estimated the valence-band offset Q_V for the investigated heterostructure. The valence-band offset has a considerable influence on the exciton binding energies and on the spin splitting as it determines the leakage of the electron and hole wave function into the nonmagnetic barriers. The condition that exciton energies of both QWs with very different well width have to be described with the same set of parameters yields a very precise value of Q_V. The energy gap of the barrier was given by its PL signal at 3.2 eV with accounting 19 meV for the exciton binding energy. Parameters used here are the effective masses of the electron $m_e/m_0=0.16$ and of the heavy hole in the growth direction $m_{\mathrm{hh},\perp}/m_0=0.74$. The fractional dimensional method[16] was applied to calculate the exciton binding energy E_X with the static dielectric constant $\epsilon_0=9.0$ and the heavy-hole in-plane mass $m_{\mathrm{hh},\parallel}/m_0=0.28$ giving values of $E_X=30$ meV and 33 meV for the QW with $L_z=52$ Å and 15 Å, respectively. The influence of strain on the band-edge energies has been included in our calculations with elastic compliance coefficients[17] and deformation potentials[18] of ZnSe. The strain affects the QW layer only because the barrier material was grown lattice matched on the GaAs substrate. The band-gap variation of the conduction band ΔE_{CB} and valence band ΔE_{VB} for different spin orientations in $Zn_{1-x}Mn_xSe$ is described by a mean-field approximation,[19]

$$\Delta E_{CB}=-N_0\alpha x\, m_s\langle S_z\rangle, \quad m_s=\pm\tfrac{1}{2}, \tag{1}$$

$$\Delta E_{\mathrm{VB}} = -\tfrac{1}{3} N_0 \beta x \, m_j \langle S_z \rangle, \quad m_j = \pm\tfrac{1}{2}, \pm\tfrac{3}{2} \tag{2}$$

with the thermal mean value of the Mn spin in the direction of the magnetic field $B = B_z$ at a temperature T,

$$\langle S_z \rangle = -S_{\mathrm{eff}} B_{5/2}\left[\frac{5 g_{Mn} \mu_B B}{2 k_B (T + T_{\mathrm{eff}})}\right]. \tag{3}$$

Bulk values of $Zn_{1-x}Mn_xSe$ for the exchange constants $N_0\alpha = 0.26$ eV and $N_0\beta = -1.31$ eV (Ref. 20) were utilized. $B_{5/2}$ represents the Brillouin function and S_{eff} (T_{eff}) alloy-dependent phenomenological parameters for the effective spin (temperature) that has been fixed to $S_{\mathrm{eff}} = 1.5$ and $T_{\mathrm{eff}} = 1.7$ K by interpolating values taken from[21] for a Mn fraction of $x = 0.05$. Despite the well width, the calulation has been performed with the same parameters for each QW. In addition to the valence-band offset, $m_{\mathrm{hh},\parallel}$ and $m_{\mathrm{hh},\perp}$ had to be varied to the above given values to obtain a fair description of the Zeeman splitting. Referring to the experimental uncertainty, we obtained a value of $Q_V = 0.22 \pm 0.04$. The calculations for the best values are shown in Fig. 3 as solid lines.

It is worth noting that the PL maximum energy of the X_{hh} luminescence originating from the 15-Å-thick QW is nearly constant up to $B = 0.6$ T and then follows the energy shift obtained from reflectance spectra with a 10 meV Stokes shift (see Fig. 4). However, in the case of the QW with $L_z = 52$ Å, both PL and reflectance show the same energy shift of the X_{hh} line over the entire range of magnetic fields. Considering that luminescence originates from localized excitons whereas reflectance scans free-exciton states, we explain such a behavior by the exciton magnetic polaron (MP) created in the narrow QW with a formation time smaller than the exciton lifetime. The MP reveals a maximum in localization energy at zero magnetic field and a continuous suppression for $B > 0$.[4] A qualitatively different energy shift of the PL signal for the two QWs is then caused by a well-width dependence of the magnetic polaron energy. In accordance to previous findings for QWs based on (CdMn)Te, the magnetic polaron is improbable in the wide QW for Mn contents below $x = 0.10$. This is due to the reduced stability of the MP for higher dimensionality (i.e., the well width) and to a less effective prelocalization of excitons in thick layers.[3] However, to support our interpretation, a more detailed investigation of MP formation in these structures is required, e.g., by the method of selective excitation.

A considerable modification of the luminescence signal for the 52-Å-thick QW has been found by exciting above the barrier energy. Under these conditions the zero-field PL spectrum is dominated by the negatively charged exciton (X^-) with the neutral exciton (X_{hh}) contributing as a high-energy shoulder as shown in Fig. 5 for an excitation energy of 4.1 eV. In magnetic fields the neutral exciton is shifted with $\Delta E_{\mathrm{CB}}(m_s = -1/2) + \Delta E_{\mathrm{VB}}(m_j = -3/2)$ to lower energies whereas the X^- line with $\Delta E_{\mathrm{VB}}(m_j = -3/2)$ only. So at a certain field X_{hh} becomes the ground state and X^- unbound. The mechanism which is similar for donor-bound excitons[22] served to identify the X^- by its suppression in magnetic fields as illustrated in the PL spectrum given in Fig. 5 for $B = 1.5$ T and by the ratio of the integral intensity $I(X^-)/I(X_{\mathrm{hh}})$ plotted in the inset as a function of magnetic field. A reason for additional electrons that are trapped by excitons to form the X^- is possibly the higher collection efficiency of electrons into the QW compared to holes due to different mobilities of the carriers created in the barrier layer.

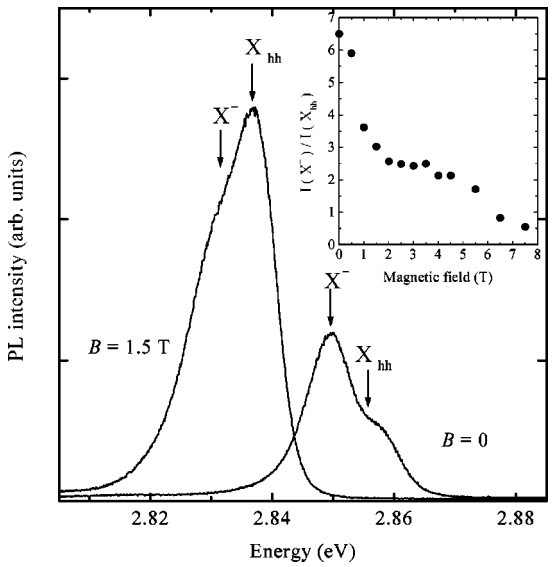

FIG. 5. PL spectra of a 52-Å-thick $Zn_{0.95}Mn_{0.05}Se/Zn_{0.76}Be_{0.08}Mg_{0.16}Se$ QW (sample *A*) excited with a photon energy of 4.1 eV above the barrier energy for zero magnetic field and $B = 1.5$ T. Inset: Ratio $I(X^-)/I(X_{\mathrm{hh}})$ of the integral X^-- to X_{hh}-exciton intensity as a function of magnetic field determined by Gaussian line-shape fits.

B. Multiple-quantum-well structures

1. Photoluminescence studies

In Figs. 6(a) and 6(b) we present PLE spectra of the $Zn_{0.91}Mn_{0.09}Se/Zn_{0.972}Be_{0.028}Se$ MQW taken at a temperature of 1.7 K for different magnetic-field strengths detected under σ^+- and σ^--polarized excitation. The strongest feature observed in the zero-field spectrum at 2.83 eV is attributed to the $1s$ state of the $e1$-hh1 exciton (denoted by X_{hh1} in Fig. 6) in the $Zn_{0.91}Mn_{0.09}Se$ wells. At 7.5 T the X_{hh1} line is split and the lower Zeeman branch is shifted by about 60 meV. As can be seen by its evolution in magnetic fields for σ^+-polarized excitation, the peak at about 2.86 eV is a superposition of several transitions, two of them with a field-induced redshift comparable to the X_{hh1} line. One can be assigned to the $e2$-hh2 state (X_{hh2}) which has been justified by a rough calculation of its energy (see the discussion below). The origin of the peak labeled $X_{\mathrm{hh}\,x}$ in Fig. 6(a) is unclear, as well as another absorption maximum appearing at 5.5 T that seems to reveal an anticrossing behavior with the X_{hh2} feature. Excited X_{hh1}-states (e.g., a $2s$ exciton) can be excluded because of the large energetic separation to the $1s$ state of about 28 meV at 7 T [the $1s$-$2s$ splitting of a 45-Å-thick QW with similar band offsets is 22 meV (Ref. 23)]. The field-independent absorption peak at 2.862 eV is ascribed to the $Zn_{0.972}Be_{0.028}Se$ barriers. By taking into account an exciton binding energy of 19 meV (the value for ZnSe) and using the alloy dependence of the $Zn_{1-x}Be_xSe$ band gap,[24] we determined the Be content to $x = 0.03$, which is in good agreement with $x = 0.028 \pm 0.003$ obtained from x-ray-diffraction analysis.

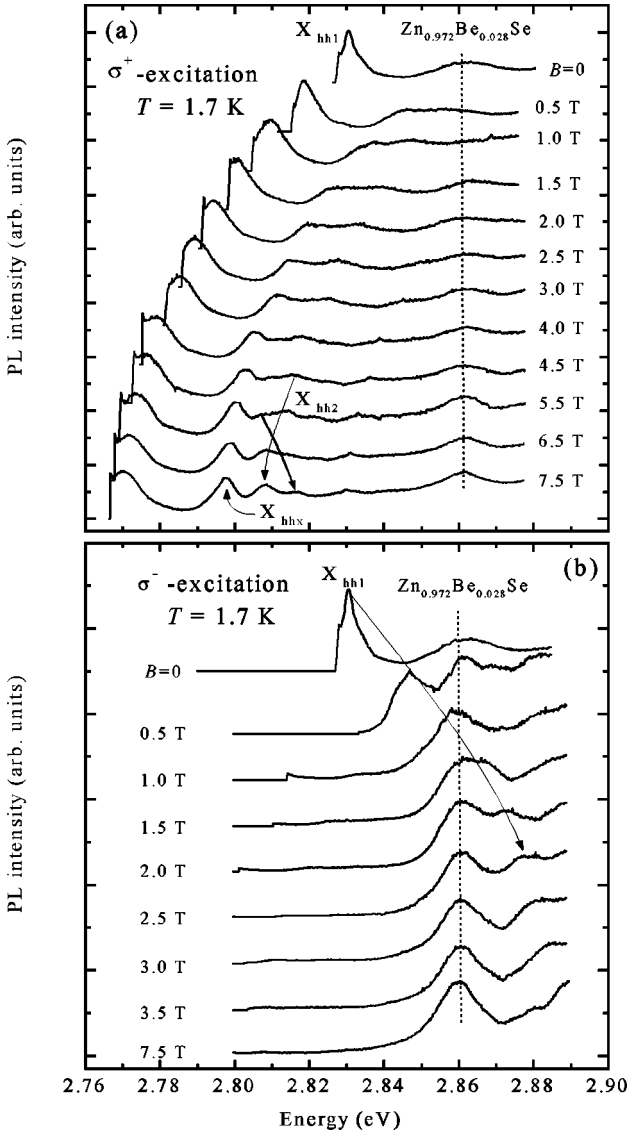

FIG. 6. PLE spectra of a $Zn_{0.91}Mn_{0.09}Se/Zn_{0.972}Be_{0.028}Se$ MQW measured under σ^+- (a) and σ^--polarized excitation (b) at 1.7 K.

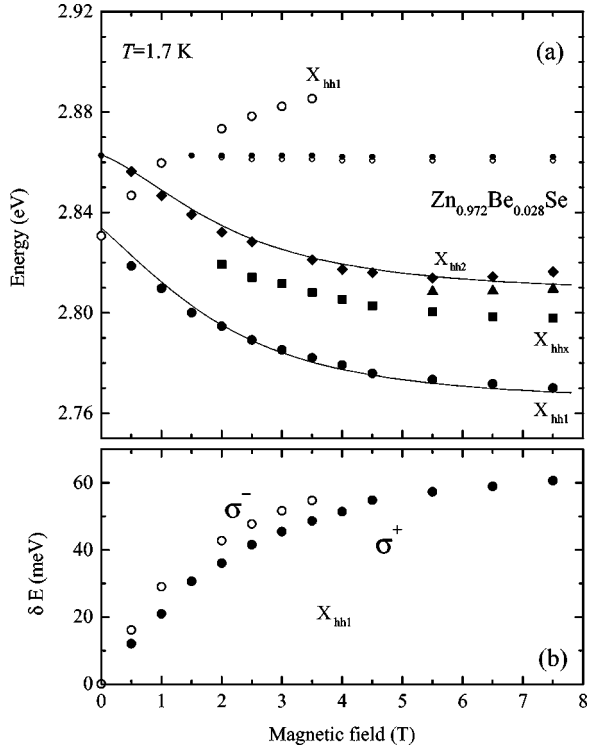

FIG. 7. (a) Exciton transition energies of a $Zn_{0.91}Mn_{0.09}Se/Zn_{0.972}Be_{0.028}Se$ MQW as a function of magnetic field (σ^+: closed symbols, crosses; σ^-: open symbols). (b) Relative spin splitting $\delta E = |E(0) - E(B)|$ of the X_{hh1} line.

As indicated in σ^--polarized absorption spectra [Fig. 6(b)], the high-energy spin state of the X_{hh1} exciton energetically meets with the barrier exciton at a critical magnetic field $B_0 = 1.5$ T at $T = 1.7$ K. In the field range $B > B_0$ for which the ground state is taken over by the barrier exciton, the further energy shift of the X_{hh1} luminescence is accompanied by its broadening and decrease of peak intensity. An indirect exciton transition which is formed by an electron and hole localized in different layers is not observed for this structure. In previous studies on SSL with nonvanishing band offset, the exchange energy of an indirect transition was found to saturate below the barrier energy[6].

Before discussing in detail, we show in Fig. 7 the PLE peak positions for the various interband transitions as a function of the magnetic field. We may point out that a perturbative approach which uses fixed single-particle wave functions to determine exciton binding energies (e.g., the fractional dimensional method applied here for single QWs) is not suitable for this MQW with small band offsets. In particular, the weak carrier confinement which is in the order of the exciton binding energy does not allow us to treat excitonic effects as a perturbation and requires a generalized variational exciton wave function for an iterative numerical solution. Moreover, the problem arises to calculate the heavy hole in-plane mass as the splitting between the heavy hole and light hole drastically changes with magnetic field (i.e., the carrier confinement). Thus we calculated the Zeeman splitting for $Q_V = 0.22$ and used the constant exciton binding energy of 20 meV for all magnetic fields to meet experimental energies (solid lines in Fig. 7). For the given reasons the calculated dependence should be regarded as an estimation only. The confinement of both electrons and holes justifies this simple approach for the lower exciton spin state, whereas it fails for the high-energy state as the Zeeman splitting of the hole leads to a type-II band alignment.

We discuss our experimental findings qualitatively with the help of a schematic band alignment for different magnetic fields shown in Fig. 8. A usual model for DMS heterostructures is applied here in which the carriers are confined in spin-dependent effective potentials generated by their exchange interaction with the magnetic system described by Eqs. (1) and (2). The total zero-field band offset has been calculated to 37 meV using the alloy dependence of the $Zn_{1-x}Mn_xSe$ and $Zn_{1-x}Be_xSe$ band gap. For σ^+-polarized $(-\frac{1}{2}, -\frac{3}{2})$-exciton transitions between electrons and heavy holes with total spin projection $m_s = -\frac{1}{2}$ and $m_j = -\frac{3}{2}$, the zero-field type I band alignment is maintained for applied magnetic fields. The giant shift of the low-energy band states which effectively increases the total band offset by about 70 meV at 7.5 T implies a continuous development from weak to strong carrier confinement for the $m_s = -\frac{1}{2}$ electrons and $m_j = -\frac{3}{2}$ holes and thus an increase in exciton oscillator

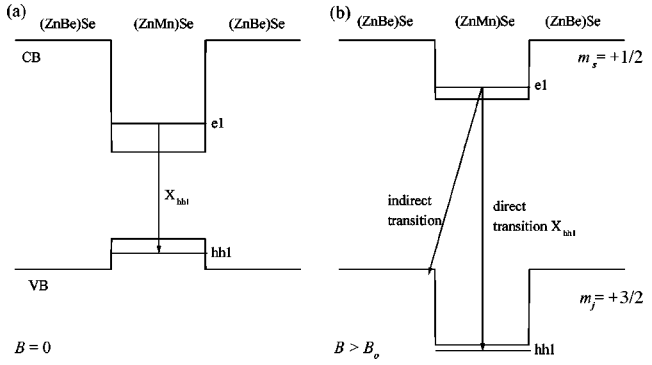

FIG. 8. Schematic alignment of the conduction (CB) and valence band (VB) in a (ZnMn)Se/(ZnBe)Se superlattice structure at zero magnetic field (a) and $B>B_0$ (b) for the electron and hole spin component $m_s=+\frac{1}{2}$ and $m_j=+\frac{3}{2}$, respectively.

strength. Experimentally this fact is displayed in PLE spectra by the $X_{\mathrm{hh}\,x}$ absorption [see Fig. 6(a)] which considerably gains in magnetic field due to the increased carrier confinement and thus enhanced overlap of the electron and hole wave function.

For $+\frac{1}{2}$ electrons and $+\frac{3}{2}$ holes, the effect of a magnetic field is to decrease the respective barrier heights. At sufficient magnetic fields in the range $0<B<B_0$, which was calculated to 0.3 T (using $Q_V=0.22$ determined for the single QWs), the small valence-band discontinuity is overcompensated by the energy shift of the heavy hole with $m_j=+\frac{3}{2}$. However, for a small negative valence-band offset the Coulomb potential generated by the electrons confined in the magnetic layers (the height of the potential for electrons is about 27 meV at 0.3 T) keeps the $m_j=+\frac{3}{2}$ holes localized in the (ZnMn)Se layer.[25] By further increasing the magnetic field, the band alignment becomes effectively type II if the heavy-hole energy in addition compensates the Coulomb potential which is about the exciton binding energy. It has been shown both experimentally[6,26] and theoretically[27] that in this case besides a spatially indirect exciton, which for our structure is composed of an electron localized in the (ZnMn)Se layer and a hole state in the nonmagnetic barrier [see Fig. 8(b)], a spatially direct exciton state can be formed. It is appropriate to regard the direct exciton as a metastable state as its energy lies above the energy of the indirect one. Although the indirect exciton is energetically favorable, its oscillator strength is small. The absorption coefficient of this state is expected to be not sufficient to give a signal in PLE measurements. Thus for the MQW under study only the direct transition is observed. A clear indication for the spin-dependent confinement is given by the spin splitting $\delta E=|E(0)-E(B)|$ of the X_{hh1} exciton, which differs for the $(-\frac{1}{2},-\frac{3}{2})$ transition (σ^+-polarized) and for the $(+\frac{1}{2},+\frac{3}{2})$ transition (σ^--polarized) shown in Fig. 7(b). Since the Zeeman splitting of band edges is symmetric, the difference in δE of about 7 meV (3 T) results from a magnetic-field-dependent exciton binding energy which increases for the lower and decreases for the upper Zeeman branch mainly caused by changes in the hole confinement.

We explain the experimentally observed weakening in the PLE maximum intensity of the $(+\frac{1}{2},+\frac{3}{2})$ transition by the broadening of the spatially direct exciton state. Two magnetic-field regimes can be distinguished in that different scattering channels contribute to the exciton broadening. In the case of a type II band alignment, the hole from the (ZnMn)Se layer can be scattered into the (ZnBe)Se barrier by the emission of acoustical phonons. The mechanism corresponds to the scattering of a metastable (spatially direct) exciton into a stable (spatially indirect) exciton. Additional scattering channels become available when the energy of the metastable exciton is shifted above the energy of the barrier exciton ($B>B_0$) and hence the well exciton as a whole can be scattered into exciton states of the nonmagnetic barriers. For the MQW under study both scattering channels are expected to get involved in the same magnetic-field range. By accounting 20 meV for the Coulomb potential (about the exciton binding energy), we estimated the band alignment to become effectively type II at $B=1.3$ T. This field almost coincides with $B_0=1.5$ T for which the energies of the barrier and well exciton are equal. The influence of scattering on the metastable exciton is further investigated by reflectance measurements to be presented in the following section. Moreover, by means of reflectance we exclude possible contributions of relaxation dynamics that may differ PLE spectra from absorption spectra.

2. Reflectivity studies

According to Eq. (3), the Zeeman splitting of band edges decreases with increasing temperature of the Mn system. Therefore, it is expected with raised sample temperature to shift the critical field B_0 to higher values where the upper Zeeman branch of the metastable QW exciton crosses the energy of the barrier exciton. We made use of this correlation to clearly identify the situation of resonant barrier and well energy in reflectance measurements.

Two series of σ^--polarized spectra taken at 1.7 K and 8 K are given in Fig. 9. The temperature of 8 K was chosen low enough to avoid changes of the band gap or thermal broadening by exciton-phonon interaction. In accordance with the energetic position in PLE spectra, the sharp feature marked in the low-temperature reflectance spectrum ($B=0$) in Fig. 9(a) is the X_{hh1} resonance. The magnetic field of 1.5 T beyond which the spectra start to be drastically altered coincides with the critical field B_0, which has been extracted from PLE measurements. As previously argued, the similar behavior is observed for the 8 K spectra shown in Fig. 9(b) at a higher critical field of B_0 (8 K) = 4.5 T. In fact in the range of X_{hh1}-exciton energies taken from PLE, which are labeled by arrows in Fig. 9(a), no significant resonance is observable. For both temperatures, the disappearance of the X_{hh1} resonance at $B>B_0$ should obviously be ascribed to the exciton scattering into barrier states. In contrast, the resonance stays pronounced in σ^+-polarized spectra, which is not discussed here.

Finally, our interpretation is confirmed by σ^--polarized reflectance spectra presented in Fig. 10 that were measured at different sample temperatures ranging from 1.7 K up to 33.5 K for a constant magnetic field of $B=7$ T, which is by far larger than B_0 (1.7 K). Up to 8 K the reflectance is barely temperature dependent. A further temperature increase causes the $(+\frac{1}{2},+\frac{3}{2})$-exciton state to meet the barrier energy, which is indicated by a significant modification of the reflectance at $T=15$ K. Despite thermal broadening, the X_{hh1} resonance is well resolved for $T>20$ K when the X_{hh1}

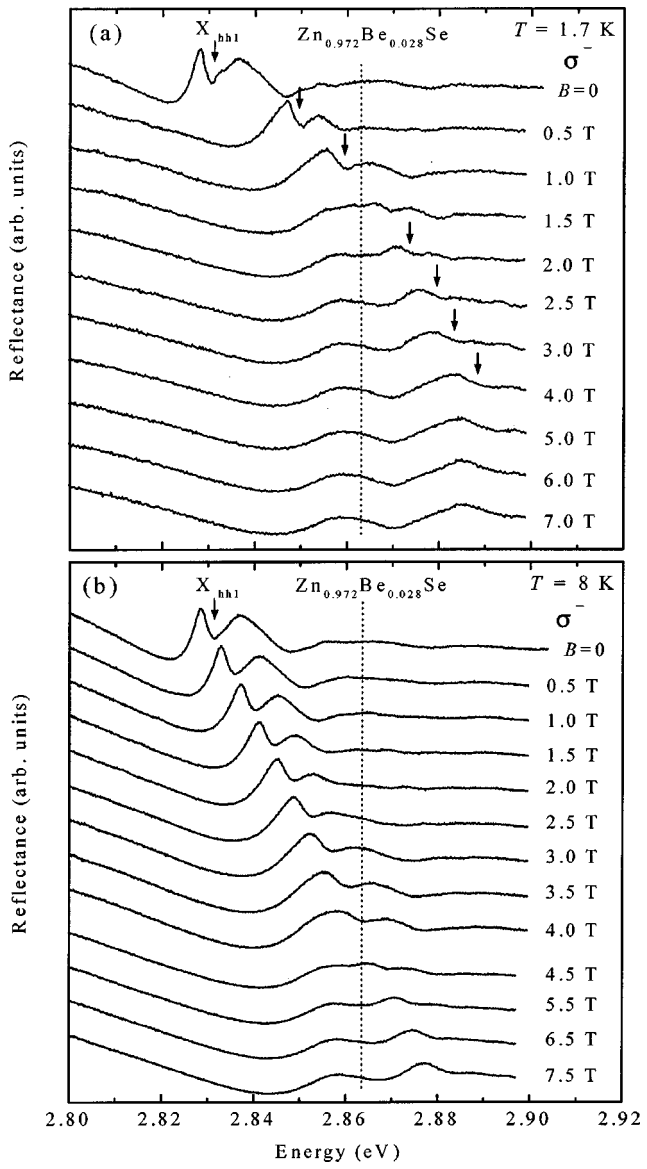

FIG. 9. σ^--polarized reflectance spectra of a $Zn_{0.91}Mn_{0.09}Se$/$Zn_{0.972}Be_{0.028}Se$ MQW taken at temperatures of 1.7 K (a) and 8 K (b). Arrows indicate X_{hh1} energies determined from PLE spectra.

state is shifted below the barrier energy and simultanuously exciton scattering into the (ZnBe)Se barriers is suppressed. The thermal broadening of the X_{hh1} feature at 33.5 K is rather strong in comparison with the spectrum for 1.7 K and 0.5 T, which reveals the exciton resonance at the same energy. A broadening for 33.5 K is unexpected since the half-width of the exicton luminescence from QWs based on binary ZnSe is barely temperature dependent up to 60 K.[28]

Experimental values for the critical field B_0 as a function of temperature are summarized in Fig. 11. The theoretical dependence for B_0 (line in Fig. 11) has been obtained in the following way. We calculated the energy shift of the $(+\frac{1}{2}, +\frac{3}{2})$ transition in magnetic fields with respect to the zero-field energy by introducing a parameter in Eqs. (1) and (2) to account for the overlap of the exciton wave function with the (ZnMn)Se layer. This parameter was varied to meet experimental points taken from PLE spectra at 1.7 K. The exchange energy for arbitrary temperatures is then determined by Eqs. (1)–(3) only with a fixed overlap parameter. The inset of Fig.

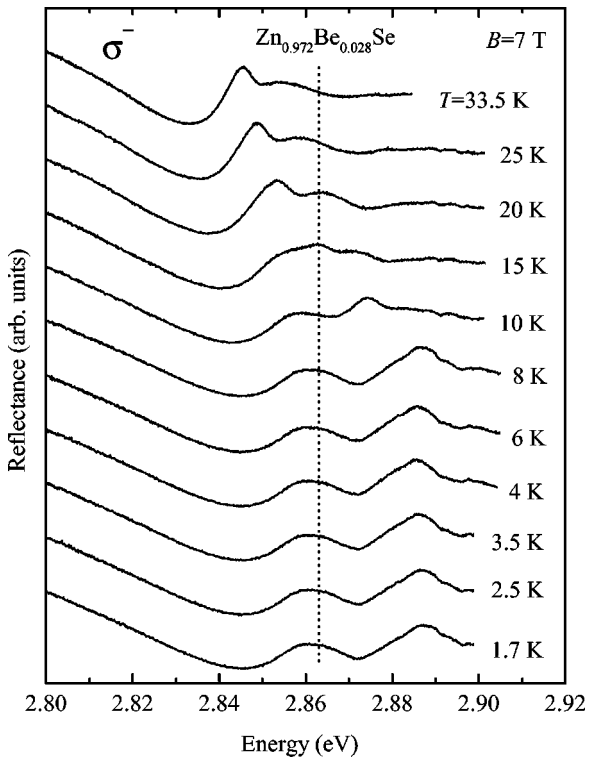

FIG. 10. Reflectance spectra of a $Zn_{0.91}Mn_{0.09}Se$/$Zn_{0.972}Be_{0.028}Se$ MQW in σ^- polarization for a series of temperatures taken at a constant magnetic field of 7 T.

11 shows the exchange energy for three temperatures that are relevant for our reflectance studies and the corresponding critical fields by arrows. With the choice of 36 meV for the exciton energy shift to meet the barrier energy (experimental value), the critical field theoretically obeys the linear shift with temperature $B_0[\mathrm{T}] = 0.44\,(T + T_{\mathrm{eff}})\,[\mathrm{K}]$, which is in

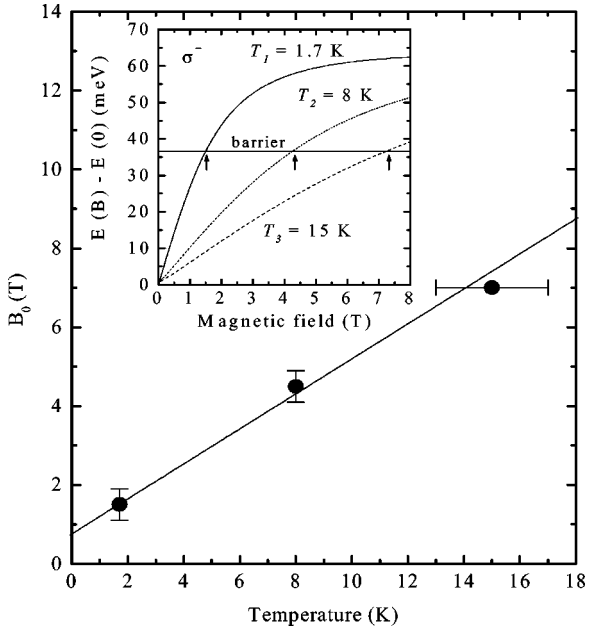

FIG. 11. Temperature dependence of the critical fields B_0 in comparison with theory (solid line). Inset: Calculated relative Zeeman splitting of the $(+\frac{1}{2}, +\frac{3}{2})$ exciton (X_{hh1}) for different temperatures. Arrows indicate B_0 for the temperatures T_i.

good agreement with our experimental findings (see Fig. 11). We note here that the linear dependence of $B_0(T)$ is not altered if changes of the exciton binding energy with magnetic fields are taken into account.

IV. CONCLUSION

We have investigated novel semimagnetic heterostructures fabricated on the basis of (ZnMn)Se/(ZnBeMg)Se by means of magnetoluminescence and magnetoreflectance spectroscopy. The valence-band offset between $Zn_{0.95}Mn_{0.05}Se$ and $Zn_{0.76}Be_{0.08}Mg_{0.16}Se$ has been determined to $Q_V = 0.22 \pm 0.04$ by a model calculation that reproduces the experimental energy shift in magnetic fields of two single quantum wells with different well widths. The formation of a spin superlattice in the valence band (i.e., type II band alignment) for one of the exciton spin states was demonstrated for a $Zn_{0.91}Mn_{0.09}Se/Zn_{0.972}Be_{0.028}Se$ multiple quantum well with a small zero-field band offset. In the regime of the spin superlattice, the absorption spectra reveal a metastable spatially direct exciton which is composed of a confined electron and a quasilocalized hole state. For sufficient magnetic fields where the barrier exciton represents the ground state of the multiple quantum well, the metastable exciton was found to be effectively broadened by scattering into excitonic barrier states.

ACKNOWLEDGMENT

This work was supported by the Deutsche Forschungsgemeinschaft through Sonderforschungsbereich 410.

*Also at A. F. Ioffe Physical-Technical Institute, Russian Academy of Science, 194021 St. Petersburg, Russia.

[1] M. A. Haase, J. Qiu, J. M. DePuydt, and H. Cheng, Appl. Phys. Lett. **59**, 1272 (1991).
[2] J. K. Furdyna, J. Appl. Phys. **64**, R29 (1988).
[3] D. R. Yakovlev, W. Ossau, G. Landwehr, R. N. Bicknell-Tassius, A. Waag, S. Schmeusser, and I. N. Uraltsev, Solid State Commun. **82**, 29 (1992).
[4] D. R. Yakovlev and K. V. Kavokin, Comments Condens. Matter Phys. **18**, 51 (1996).
[5] R. B. Bylsma, W. M. Becker, J. Kossut, U. Debska, and D. Yoder-Short, Phys. Rev. B **33**, 8207 (1986).
[6] W. Y. Yu, M. S. Salib, A. Petrou, B. T. Jonker, and J. Warnock, Phys. Rev. B **55**, 1602 (1997).
[7] A. Waag, Th. Litz, F. Fischer, H.-J. Lugauer, T. Baron, K. Schüll, U. Zehnder, T. Gerhard, U. Lunz, M. Keim, G. Reuscher, G. Landwehr, in *Festkörperprobleme/Advances in Solid State Physics*, edited by R. Helbig (Vieweg, Braunschweig/Wiesbaden, 1998), Vol. 37, p. 43.
[8] A. Waag, F. Fischer, K. Schüll, T. Baron, H.-J. Lugauer, Th. Litz, U. Zehnder, W. Ossau, T. Gerhard, M. Keim, G. Reuscher, and G. Landwehr, Appl. Phys. Lett. **70**, 280 (1997).
[9] M. von Ortenberg, Phys. Rev. Lett. **49**, 1041 (1982).
[10] W. Ossau, B. Kuhn-Heinrich, G. Mackh, A. Waag, and G. Landwehr, J. Cryst. Growth **159**, 1052 (1996).
[11] N. Dai, H. Luo, F. C. Zhang, N. Samarth, M. Dobrowolska, and J. K. Furdyna, Phys. Rev. Lett. **67**, 3824 (1991).
[12] W. C. Chou, A. Petrou, J. Warnock, and B. T. Jonker, Phys. Rev. Lett. **67**, 3820 (1991).
[13] B. T. Jonker, H. Abad, L. P. Fu, W. Y. Yu, A. Petrou, and J. Warnock, J. Appl. Phys. **75**, 5725 (1994).
[14] S. Takagi, J. Phys. Soc. Jpn. **26**, 1239 (1969).
[15] M. Nawrocki, Yu. G. Rubo, J. P. Lascaray, and D. Coquillat, Phys. Rev. B **52**, R2241 (1995).
[16] P. Christol, P. Lefebvre, and H. Mathieu, J. Appl. Phys. **74**, 5626 (1993).
[17] D. Berlincourt, H. Jaffe, and L. R. Shiozawa, Phys. Rev. **129**, 1009 (1963).
[18] B. Rockwell, H. R. Chandrasekhar, M. Chandrasekhar, A. K. Ramdas, M. Kobayashi, and R. L. Gunshor, Phys. Rev. B **44**, 11 307 (1991).
[19] J. A. Gaj, R. Planel, and G. Fishman, Solid State Commun. **29**, 435 (1979).
[20] A. Twardowski, M. von Ortenberg, M. Demianiuk, and R. Panthenet, Solid State Commun. **51**, 849 (1984).
[21] W. Y. Yu, A. Twardowski, L. P. Fu, A. Petrou, and B. T. Jonker, Phys. Rev. B **51**, 9722 (1995).
[22] D. Heiman, P. Becla, R. Kershaw, D. Ridgley, K. Dwight, A. Wold, and R. R. Galazka, Phys. Rev. B **34**, 3961 (1986).
[23] W. Ossau, D. R. Yakovlev, U. Zehnder, G. V. Astakhov, A. V. Platonov, V. P. Kochereshko, J. Nürnberger, W. Faschinger, M. Keim, A. Waag, G. Landwehr, P. C. M. Christianen, J. C. Maan, N. A. Gippius, and S. G. Tikhodeev, Physica B **256-258**, 323 (1998).
[24] V. Wagner (private communication).
[25] A. V. Kavokin, V. P. Kochereshko, G. P. Posina, I. N. Uraltsev, D. R. Yakovlev, G. Landwehr, R. N. Bicknell-Tassius, and A. Waag, Phys. Rev. B **46**, 9788 (1992).
[26] W. Y. Yu, S. Stoltz, A. Petrou, J. Warnock, and B. T. Jonker, Phys. Rev. B **56**, 6862 (1997).
[27] J. Warnock, B. T. Jonker, A. Petrou, W. C. Chou, and X. Liu, Phys. Rev. B **48**, 17 321 (1993).
[28] L. Malikova, W. Krystek, F. H. Pollak, N. Dai, A. Cavus, and M. C. Tamargo, Phys. Rev. B **54**, 1819 (1996).